CO4-1 Millimeter Wave Absorption Spectra of Ionic Liquids

T. Awano and T. Takahashi[1]

Faculty of Engineering, Tohoku Gakuin University
[1]Research Reactor Institute, Kyoto University

INTRODUCTION: We have observed millimeter wave absorption bands of AgI-superionic conductive glasses in sub-terahertz region. We also observed these absorption bands in CuI-superionic conductive glasses[1-3]. These bands seem to be due to collective motion of the conductive ions because their frequencies are lower than those estimated from the ionic masses. However, the dynamics of the collective movement of ions is not clear yet.

Ionic liquids(ILs) are molten salts even at room temperature because of large and anisotropic radius of composing anions and cations. It is interesting to compare ionic motion in the ILs with those in superionic conductor for making clear the effect of glass network structure onto the collective movement of ions.

Recently, we have observed sub-terahertz absorption bands of ILs[4-6]. These bands seem to be due to ionic movement because of their temperature dependence. That is to say, the absorption bands disappear at low temperatures at which the IL is solid. However, the thermal change of absorption spectra of these ILs were in various way. This difference seems to be due to the difference of the process of their phase transition to the solid states (crystal or glass).

In this study we have measured millimeter wave absorption spectra of 33 ILs to make clear the ionic movement from the temperature change of absorption spectra.

EXPERIMENTS: A fixed amount of ionic liquids (Tokyo Chemical Industry Co., Ltd.) were spread into filter paper. Transmission spectra of single and double papers with ionic liquids were measured at room temperature and low temperatures. Absorption spectra were obtained by subtraction of them. To confirmation, measurements were repeated two or three times for each IL. Molecular dynamics simulation is executed by Gromacs 5.0.

RESULTS: Four types of the spectral change occurred at temperature above melting point or glass transition temperature[7]. The intensities of the absorption bands in the ILs which are crystal in the solid state showed rapid decrease at their melting points[4,5]. On the other hand, those in ILs which are vitreous in the solid state weakened and shifted gradually. Some others showed complicated change. The other type showed no absorption band in this spectral range. Figures 1.a-d show typical spectra of these four types. Origin of these difference is not clear yet. To investigate these variety of spectra, molecular dynamics simulation is underway.

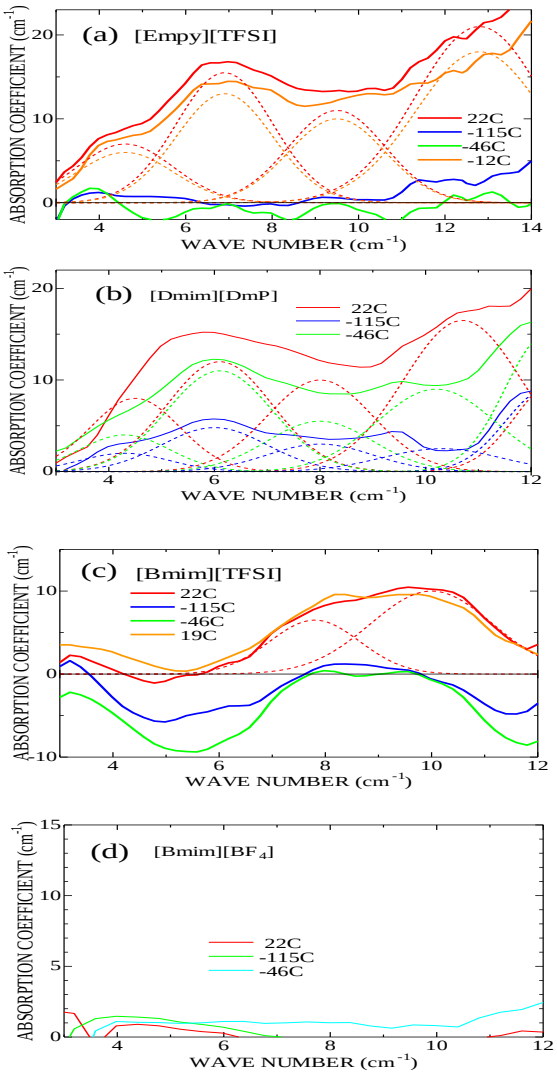

Fig. 1. Typical temperature dependence of absorption increment spectra of ionic liquids. The baseline is the absorption spectrum at 88 K.

REFERENCES:

[1] T. Awano and T. Takahashi, J. Phys. Conf., **148** (2009) 012040/1-4.
[2] T. Awano and T. Takahashi, J. Phys. Soc. Jpn. **79** Suppl. A (2010) 118-121.
[3] T. Awano and T. Takahashi, Proceedings of the 13th Asian Conference on Solid State Ionics, (2012) 569-576.
[4] T. Awano and T. Takahashi, KURRI Progress Report 2014, CO4-2.
[5] T. Awano , A. Shikoda and T. Takahashi, 20th International Conference on Solid State Ionics, (2015) D2.02.
[6] T. Awano and T. Takahashi, KURRI Progress Report 2015, CO4-1.
[7] T. Awano , A. Shikoda and T. Takahashi, 21th International Conference on Solid State Ionics, (2017) IV-6 P.

CO4-2 Synthesis of Noble Metal Nanoparticles Supported on Graphene by Irradiation Reduction Method

F.Hori, H.Nakanishi, A.Tokai, M.Tanaka, S.Toda, M.Tani, A.Iwase, K.Okitsu, Y.Mizukoshi[1] and Q.Xu[2]

Dept. of Mater. Sci., Osaka Prefecture University
[1]*Institute of Materials Research, Tohoku University*
[2]*Research Reactor Institute, Kyoto University*

INTRODUCTION: Metallic nanoparticles have some specific properties, which are not appeared in bulk materials such as catalytic activities, magnetic properties, electro conductivity and light absorption. These properties depend on its size, shape, structure, chemical composition and so on. They have many possibilities to applied for various industrial fields. However, it is not easy to fabricate multi elemental alloy nanoparticles with controlling their size, shape and structure. Generally, many kinds of metal nanoparticles commercially are synthesized by using chemical reaction method, which is not necessarily in water solution. Recent years, some reports show that it is possible to fabricate various metal nanoparticles under irradiation reduction fields such as ultrasonic, solution plasma, electron beam, ion beam and gamma-ray irradiation. So far, we have tried and reported that synthesis of shape and size controlled Au, Ag, Pd, Pt, Cu and their complex nanoparticles under irradiation reduction fields. On the other hand, we have developed a one-step gamma-ray irradiation method to synthesize nanocomposites composed of graphene and Pt nanoparticles from aqueous solution containing graphene and Pt ions in water [1]. In this study, we have tried to synthesize nanocomposites composed of graphene (Gp) and Pd nanoparticles (NPs) in aqueous solution by gamma-ray irradiation, electron beam irradiation.

EXPERIMENTS: Aqueous solutions with a given concentration of Pd(II) ($PdCl_2 \cdot 2NaCl \cdot 3H_2O$) and 2-propanol. Graphenepowder (6 - 8 nm thick x 5 μm wide) was added into this water solution. The solution was argon gas purged and sealed into polystyrene vessels. After dispersion by an ultrasonic cleaning bath, they were irradiated at about 300 K with γ-rays from ^{60}Co radio active source at gamma irradiation facility in KURRI, Kyoto University. The total dose was fixed to 10 kGy with dose rate of 13.6 kGy/h. After irradiation, the products were separated by centrifugation, washed with water and dried by freeze-drying. UV–vis absorption spectra were measured and all products were observed by conventional TEM. Infrared spectra and Raman spectra (RS) of the prepared samples were collected by a Fourier-transform infrared spectro-photometer (FT-IR) and a Raman spectrophotometer.

RESULTS:
Pd NPs supported on Gp (Pd/Gp) were formed in one-pot aqueous solution containing Gp and Pd(II) complex ions by gamma-ray or electron beam irradiation. As shown in figure 1, it was confirmed that gamma-ray and electron beam irradiation provided carbonyl groups (C=O) on Gp and Pd NPs formed from the radiolytic reduction of Pd(II) complex ions were supported on the carbonyl modified Gp. Although there is no fundamental difference in the reaction generated by gamma-ray and electron beam irradiation, but the size of Pd NPs of Pd/G was differed greatly between them. Furthermore, Pd NPs supported on nitrogen-doped Gp (Pd/N-Gp) were prepared by the same condition of gamma-ray and electron beam irradiation. The size of the Pd NPs of Pd/N-Gp was smaller than that of Pd/G because of the increased number of adsorption sites of Pd NPs.

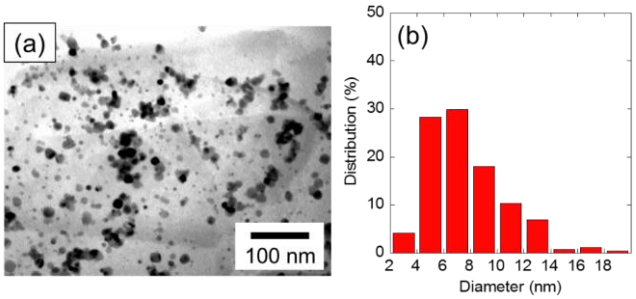

Fig. 1 TEM image and size distribution of Pd-NPs supported on graphene synthesized under gamma-ray irradiation field.

Acknowledgement
This work was supported by JSPS KAKENHI Grant-in-Aid for Scientific Research (A)-15H02342.

Reference
[1] A.Tokai, K.Okitsu, F.Hori, Y.Mizukoshi, A.Iwase, Rad. Phys. Chem. 123, (2016) 68-72

CO4-3 Electron Irradiation Induced Damage Structure in Intermetallic Alloys

F. Hori, Y. Ueno, Y. Sumikura, K. Kobayashi, A. Iwase, K. Ohsawa[1], Q. Xu[2] and N. Abe[2]

Dept. of Mater. Sci., Osaka Prefecture University
[1]Res. Inst. of Appl. Mech., Kyushu University
[2]Res. Reactor Inst., Kyoto University

INTRODUCTION: Fe-Al compound alloys have good properties such as specific strength to weight ratio, oxidation resistance and strength in elevated temperature. It is well known that intermetallic compound alloys possibly include more than two types of vacancies basically, that is A-vacancy and B-vacancy in A-B compound alloy. Thermally equilibrium defects and chemically deviated structural defects in these compound alloys are very complicated. However, the amount of defect and the defect structure affects the various characteristic features, such as strength and electronic conductivity and so on. Moreover, first principle calculation shows that different number of hydrogen atoms can be trapped by Al- or Fe-vacancy in B2 type Fe-Al alloy. On the other hand, we have reported that vacancies introduced by electron irradiation strongly depend on electron energy because of their different threshold energy of displacement for each elemental atom. Then we supposed that radiation induced vacancy type defects can be controlled by changing the energy of electron irradiation. In this study, we have performed electron irradiation for Fe-Al alloys followed by hydrogen charging by electrochemical method and H+ ion implantation. After irradiation and hydrogen charging into Fe-Al alloys, Thermal desorption spectrometry (TDS) and positron annihilation measurements were carried out.

EXPERIMENTS: Fe-48%Al alloy specimens with B2 structure were prepared by arc melting method. Sliced samples with the thickness of 0.5 mm were annealed at 973 K for 120 h followed by air-quenched in vacuum. These specimens were irradiated with 2 MeV electron to the fluence of 1×10^{17} and 1×10^{18} /cm^2 at JAEA-Takasaki and with 9 MeV electron to the fluence of 5×10^{17} and 3×10^{18} /cm^2 at KURRI, Kyoto University. In both cases, irradiations were carried out at about 330 K controlled by water flow system. After electron irradiation, hydrogen atoms were cathodically charged in the sulfuric acid aqueous solution including NH_4SCN as an additive. Also 1.5 MeV-H^+ irradiation with the fluence of 1×10^{16} ions/cm^2 have performed for these alloys at National Institute for Quantum and Radiological Science and Technology. After and before irradiation, samples were examined by X-ray diffraction, positron annihilation lifetime, coincidence Doppler broadening measurements and TDS. The positron lifetime spectra were analyzed by using POSITRONFIT program.

RESULTS: After electro-chemical charging and hydrogen implantation into Fe-Al alloys, some peaks observed in TDS spectra representing emission of decomposed hydrogen bounded by defects and grain boundary (Fig.1). It found that hydrogen released temperature for electron irradiated sample followed by hydrogen charging is slightly higher than that for hydrogen charged sample without irradiation. This result reveals that the introduced hydrogen atoms might be trapped by vacancy. On the other hand, positron annihilation Doppler broadening S parameter decreases after hydrogen charging or H^+ irradiation showing that implanted hydrogen is trapped by vacancy. This result is consistent with the results of TDS.

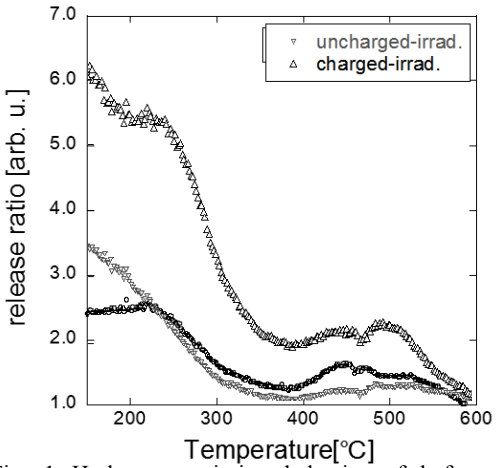

Fig. 1 Hydrogen emission behavior of before and after irradiated Fe-Al alloys.

Acknowledgement
This work was supported by JSPS KAKENHI Grant-in-Aid for Scientific Research (B)-26289365.

CO4-4 Observation of Transient Damage States in Materials under Ion Irradiation

H. Tsuchida[1,2], H. Minagawa[2], S. Nakanishi[2] and Q. Xu[3]

[1]*Quantum Science and Engineering Center, Kyoto University*
[2]*Department of Nuclear Engineering, Kyoto University*
[3]*Research Reactor Institute, Kyoto University*

INTRODUCTION: The effects of energetic-particle irradiation on metallic materials have been extensively studied in nuclear and radiation materials science. Ion irradiation induces crystal lattice disorder following various dynamic relaxation processes including defect recombination and aggregation. During irradiation, damage evolution proceeds by the reciprocal processes of defect production and relaxation, and then reaches a certain equilibrium damage state. To date, experimental and computer simulation studies have focused on an understanding of a transient damage state under irradiation, and a new model calculation relevant to dynamic annealing has recently been reported [1].

To understand transient damage states in materials under ion irradiation, we performed in situ X-ray diffraction (XRD) study of lattice expansion associated with deformation of a thin Al foil under MeV-energy heavy-ion irradiation [2]. The change in the lattice parameter during irradiation and its ion-beam flux dependence were analyzed. We investigated the effect of defect production on lattice expansion. Moreover, with the correlation between lattice expansion and displacement damage, we considered a model for lattice expansion originating from the accumulation of Frenkel defects. From the model, we obtained the relationship between the relative change in lattice parameter and the value of displacement per atom (dpa) rate. A comparison of the results from model calculations and experiments shows that the dpa rate calculated from the model, which takes account of athermal defect-recombination, is strongly correlated with the change on lattice parameter. This result suggests that the concentration of surviving defects under irradiation diminishes because of spontaneous recombination of defect produced.

EXPERIMENTS: A high-purity well-annealed aluminum foil with a thickness of 3 μm was used as a target specimen. The free-standing target foil was irradiated with three different projectiles: specifically 2.5-MeV C, 3.0-MeV O and 4.3-MeV Si ions. We performed in situ X-ray diffraction (XRD) analysis of the target specimen under ion irradiation, and measured diffraction peak from Al (200) plane before, during and after ion irradiation.

RESULTS: During ion irradiation, the diffraction peak position was sifted to a lower diffraction angle compared with that measured before irradiation, indicating an expansion of lattice. The relative change in lattice parameter, $\Delta a/a = \left(a_{during} - a_0\right)/a_0$, increases as the beam flux increases, where a_0 and a_{during} are the lattice constant observed before and during irradiation, respectively. Fig. 1 shows the dependence of dpa rate on the relative change in the lattice parameter. The dpa rate is given as $\sigma_d^{arc} \times \phi$, where σ_d^{arc} is the displacement damage cross section estimated using the athermal recombination-corrected (*arc*) model [3], and ϕ is the beam flux. The *arc* model was developed to estimate the damage cross sections taking account of athermal defect-recombination. This enables the determination of the surviving fraction or the recombination fraction of defects produced during irradiation. The result indicates that the magnitude of the lattice expansion is correlated with the *arc*-dpa rate. Thus, the present in situ XRD experiment affords a new method to investigate transient damage states in materials under ion irradiation.

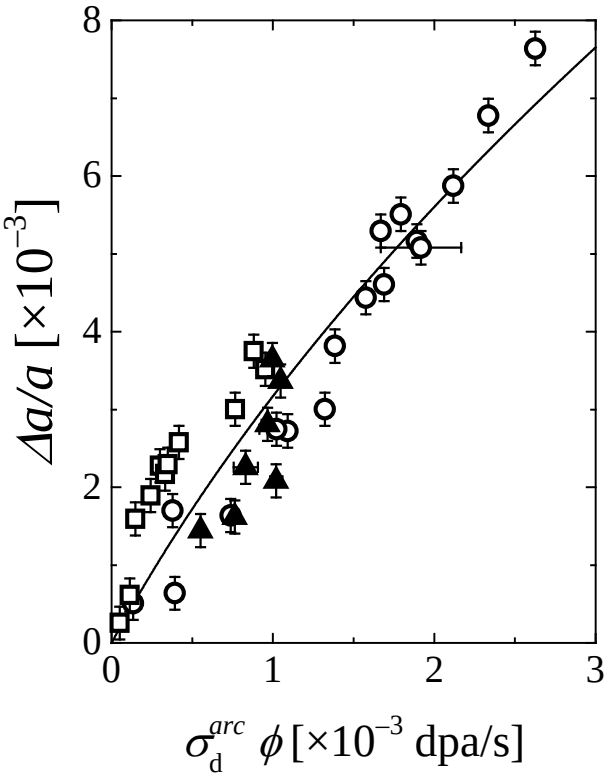

Fig. 1. Dependence of the relative change of the lattice parameter on the dpa rate. Symbols denote the experimental data: □ for 2.5-MeV C ions, ▲ for 3.0-MeV O ions, and ○ for 4.3-MeV Si ions. Solid curve denotes a result of fitting the data.

REFERENCES:

[1] X.M. Bai *et al.*, Science, **327** (2010) 1631-1634.
[2] M. Minagawa *et al.*, Nucl. Instr. and Meth. B, **372** (2016) 38-43.
[3] K. Nordlund et al., Nucl. Sci. NEA/NSC/DOC (2015) 9.

CO4-5 Trapping of Hydrogen Isotopes at Vacancy-Type Defects in Tungsten

Y. Hatano, K. Yumizuru[1], T. Toyama[2] and Q. Xu[3]

Hydrogen Isotope Research Center, Organization for Promotion of Research, University of Toyama
[1]Graduate School of Science and Engineering for Education, University of Toyama
[2]Institute for Materials Research, Tohoku University
[3]Research Reactor Institute, Kyoto University

INTRODUCTION: Retention of hydrogen isotopes especially tritium in plasma facing materials is one of the most important issues in safety assessment of fusion reactors. It has been shown that neutron irradiation causes significant increase in deuterium (D) retention in W, a leading candidate of plasma-facing material, due to trapping effects of radiation-induced defects [1]. Detailed understanding of trapping mechanisms is necessary for the mitigation of this undesirable irradiation effects.

To examine defect-hydrogen isotope interactions in W, the authors irradiated samples of polycrystalline W with high energy electrons to 10^{-3} dpa to induce Frenkel pairs uniformly throughout the bulk [2]. Then the irradiated samples were annealed at 573 K under vacuum or D_2 gas atmosphere, and clustering of vacancy-type defects and D trapping were examined using positron annihilation spectroscopy (PAS) and thermal desorption spectroscopy (TDS) [2]. Significant increase in positron lifetime accompanied with increase in D retention was observed after electron irradiation and subsequent annealing due to formation of vacancies and their clustering. In addition, positron lifetime for D-charged samples was shorter than that for D-free samples annealed in vacuum. This difference was ascribed to the presence of electrons of D atoms in vacancies.

In this year, detailed coincidence Doppler broadening (CDB) measurements were performed for better understanding of D trapping at vacancy clusters. Samples irradiated to lower dose were also examined to clarify the threshold damage level at which the irradiation effects on hydrogen isotope retention starts to appear.

EXPERIMENTS: Disk samples of W were irradiated with 8.5 MeV electrons to $\sim 1 \times 10^{-3}$ dpa at LINAC at Kyoto University Research Reactor Institute (KURRI). The irradiated samples were shipped to International Research Center for Nuclear Materials Science, Institute for Materials Research (IMR-Oarai), Tohoku University. A part of samples were sealed into quartz capsules under vacuum or D_2 gas atmosphere (0.1 MPa) and heated at 573 K for 100 h. Then CDB measurements were performed using ^{22}Na positron source.

Several W samples were irradiated with 5.5 MeV electrons at LINAC at KURRI to $\sim 5 \times 10^{-4}$ dpa. Positron lifetime and D retention after exposure to D plasma at 450 K were measured.

RESULTS AND DISCUSSION: Fig. 1 shows ratio curves of CDB spectra obtained by normalizing each CDB spectrum to that of well-annealed W sample. The electron irradiation and subsequent annealing in vacuum resulted in clear increase in the ratio values in the low momentum region and decrease in the high momentum region. This change indicates increase in the probability of positron annihilation with conduction electrons due to formation and clustering of vacancies. The presence of D in the samples led to further increase in the ratio values in the low momentum region and decrease in the high momentum region. The remarkable influence of D is explained by annihilation of positrons with valence electrons of D atoms in vacancies. In other words, the observed change in the ratio curve is one of the direct evidences of D trapping at vacancies.

The positron life time for W samples irradiated to $\sim 5 \times 10^{-4}$ dpa was 117.9 ± 0.4 ps. This value is comparable with that for non-irradiated W (118 ps). No clear effects on D retention was observed. It was therefore concluded that irradiation effects on hydrogen isotope retention becomes significant at $\sim 10^{-3}$ dpa.

CDB measurements were performed under the framework of Joint Research of IMR-Oarai.

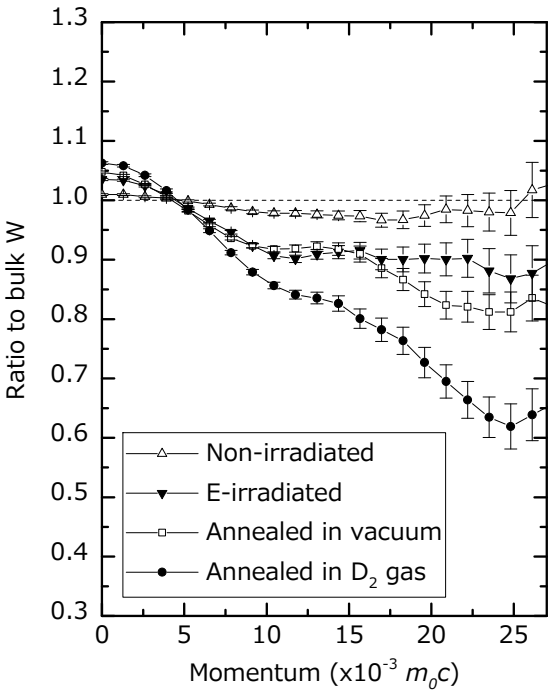

Fig. 1 Ratio curves of CDB spectra of non-irradiated W and those after electron irradiation and subsequent annealing at 573 K under vacuum or D_2 gas atmosphere (0.1 MPa). The curves were obtained by normalizing each CDB spectrum to that of well-annealed W samples.

REFERENCES:

[1] Y. Hatano *et al.*, J. Nucl. Mater., **438** (2013) S114–S119 and Nucl. Fusion **53** (2013) 07300
[2] Y. Hatano *et al.*, KURRI Progress Report 2015, 81

CO4-6 Preliminary Study of Variation in Current-Voltage Characteristics of Field Emitter Array Structure under Gamma-ray Irradiation

Y. Gotoh, T. Morito, M. Nagao[1], N. Sato[2], M. Akiyoshi[3], and I. Takagi

Graduate School of Engineering, Kyoto University
[1]National Institute of Advanced Industrial Science and Technology, AIST
[2]Research Reactor Institute, Kyoto University
[3]Radiation Research Center, Osaka Prefecture University

INTRODUCTION: We have been investigating radiation tolerance of the components of a compact image sensor based on field emitter array (FEA) and photoconductor [1,2]. The purpose of the development is to realize a compact image sensor that can be used for the nuclear decommissioning process for Fukushima Daiichi nuclear power plant. By the last year, we have irradiated gamma-ray to the FEAs and cadmium telluride-based photodiodes to check the robustness of these devices. As a result, the properties of these devices were not deteriorated with the γ-ray irradiation until the adsorbed dose reached 1.2 MGy [1]. Now the research phase is moved to the next stage where *in situ* observation of the device performance under γ-ray irradiation. Last year, we have made the first preliminary experiments of the *in situ* observation [3]. However, the method of the measurements has not yet been established. In this study, we have performed a similar experiments, but irradiating the FEA sample from oblique direction.

EXPERIMENTAL SETUP: The measurements of the current-voltage characteristics were made in a small vacuum vessel that was evacuated before the irradiation experiments. The vacuum vessel was connected with a separate vacuum pumping system via a 1/4" stainless steel tube. The vessel itself did not possessed a pumping system. Therefore, the vessel was once evacuated by a vacuum system connected to the vessel, and the vessel was then encapsulated to be irradiated by γ-rays.

EXPERIMENTAL PROCEDURE: The FEAs were fabricated at National Institute of Advanced Industrial Science and Technology. Since the FEAs possessed three electrodes of emitter, gate and focus, the current that flowed these electrodes were monitored with a source-measure units. In the previous measurement, irradiation of γ-ray was performed from the normal direction of the FEA surface. In the present study, irradiation was performed from the side to observe the effect of the γ-ray incidence. The measurements were done at two different distances from the γ-ray source: 22 cm and 40 cm.

RESULTS: Figure 1 shows the current-voltage characteristics of the emitter, gate, and focus electrodes under γ-ray irradiation, measured at 22 cm distant from the γ-ray source. When the emitter was biased to -5 V, the emitter current of about -4 nA was observed. While the gate and focus currents were about 1.5 nA and sum of these currents approximately coincides the value of the emitter current. The electric resistance was calculated to be about 1 GΩ, which was approximately the same value obtained in the previous measurement. The data acquired at the distance of 40 cm showed similar values.

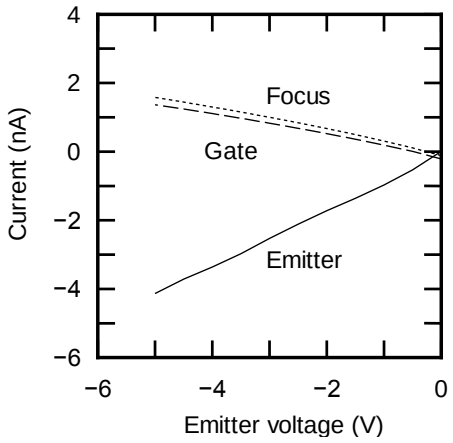

Fig. 1. Current-voltage characteristics of the emitter, gate, and focus electrodes under the γ-ray irradiation.

DISCUSSION: In the FEA, the emitter was common and the upper electrode was either the gate or the focus electrode. The ratio of the areas corresponding to the gate and the focus is not unity, it was somewhat strange to have similar currents between the gate and the focus. One possible reason for this would be the effect of the leads from the feedthrough to the device. Shielding the lead may be necessary.

SUMMARY: The current-voltage characteristics of FEAs under the γ-ray irradiation were measured. The emitter current was larger than the gate and the focus electrodes. Detailed analysis of these currents are now underway.

ACKNOWLEDGMENTS: A part of this study was supported by Japan Society for Promotion of Science through a Grant-in-Aid for Scientific Research No. 16H04631.

REFERENCES:

[1] Y. Gotoh *et al.*, Tech. Dig. of the 29th International Vacuum Nanoelectronics Conference, IVNC2016, Vancouver, July 8-10, 2016, p. 20.
[2] T. Okamoto *et al.*, Physica Status Solidi (c) **13** (2016) 635.
[3] Y. Gotoh *et al.*, KURRI Progress Report 2015 (2016) p. 73

CO4-7 Study of the Properties of Water and the Physiological Activation Phenomena by using High-Intensity Pulsed Coherent Radiation

S. Okuda, Y. Tanaka, Y. Kida and T. Takahashi[1]

Graduate School of Engineering, Osaka Prefecture University
[1]Research Reactor Institute, Kyoto University

INTRODUCTION: The coherent transition radiation (CTR) from electron bunches of a linear accelerator (linac) has continuous spectra in a submillimeter to millimeter wavelength range corresponding to the terahertz (THz) frequency range. It is a picosecond pulsed light and hence, has extremely high peak-intensities compared with the other THz light sources. The light source system using the CTR from the electron beams of the 45 MeV L-band electron linac was established at Kyoto University Research Reactor Institute (KURRI) [1-3]. This CTR light source developed has been applied to absorption spectroscopy. Recently, the possibility of any nonlinear effects was found in the measurement of the absorption spectroscopy at KURRI.

The important application of the light source is the investigation of the biological effects of the CTR. The main purpose of the present work is the investigation of the biological effects of the high-intensity pulsed CTR.

EXPERIMENTAL METHOD: The electron linac at KURRI was used in the experiments. In most experiments the beam energy, macropulse length and the repetition rate are 42 MeV, 47 ns and 60 Hz, respectively. The experimental configurations for the absorption spectroscopy are schematically shown in Fig. 1. The output CTR light from a light source chamber was transported out from the accelerator room. The spectrum of the light after passing through the sample was measured with a Martin-Puplett type interferometer and a liquid-He-cooled silicon bolometer. The wavenumber resolution was 0.1 cm^{-1}. The incident light was divided to two parts with the same light intensity in the interferometer. In this system the absorption spectroscopy and the irradiation were carried out at the same time.

In the absorption spectroscopy the sample was located on the light path between the interferometer and the detector. The thickness of the liquid sample was about 100 μm, which was sandwiched with two anhydrous quartz plates 3 mm thick. The light was focused at a light collimator 8 mmϕ in diameter located before the sample. The details of the methods for the measurements are described in ref. 2 and 3. The liquid samples used in the experiments were water, aqueous solutions of NaCl for the investigation of the basic behaviors of the absorbed light in the analysis of the biological effects by the irradiation of CTR.

In the irradiation experiments of the CTR several kinds of bacillus, cell and microorganism were used. After the irradiation the physiological activation phenomena were investigated. The new system for observing the sample during the CTR irradiation experiments is under preparation.

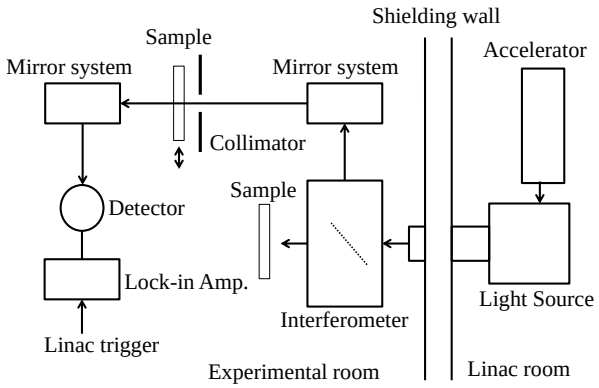

Fig. 1. Schematic diagram showing the configurations for absorption spectroscopy and irradiation experiments using the CTR

RESULTS AND DISCUSSION: The characteristics of the CTR light source were investigated, and the electron beam conditions and the experimental configurations were optimized. The light spectrum was sufficiently stable during the measurements within ±2-3% in a wavenumber range of 4-13 cm^{-1}. The spectrum had a peak at a wavenumber of about 7 cm^{-1}. If a band-pass light filter or a grating-type monochromator is used in order to avoid the influence of the main part of the spectrum around the peak the wavenumber range would be expanded to 2-35 cm^{-1}, which is determined by the specification of the detector. The intensity of light was estimated to be about 10^{-7} W/0.1%b.w. and was found to be sufficiently high even if it becomes 10^{-6} of the initial one after transmission through the sample due to absorption. The micropulse length of the CTR which corresponds to that of the electron beam from the linac was evaluated by the interferogram to be about 3 ps. Such a relatively short pulse length is due to the special bunching process in the optimized operational conditions of the linac. These results indicate that the peak light intensity in the micropulse is about 10^4 W. While the averaged CTR power is sufficiently low to induce thermal effects, the comparatively high peak power might cause any nonlinear effects.

In the irradiation experiments of CTR to investigate the biological effects the experimental conditions have been optimized. Preliminary results have been obtained by the CTR irradiation so far.

REFERENCES:

[1] T. Takahashi et al., Rev. Sci. Instrum. **69** (1998) 3770.
[2] S. Okuda and T. Takahashi, Infrared Phys. Technol. **51** (2008) 410.
[3] S. Okuda and T. Takahashi, J. Jpn. Soc. Infrared Science & Technology 25 (2016) 49 (in Japanese).

CO4-8 Spectrum of Amino Acid in the Sub-THz region using Coherent TR

T. Takahashi

Research Reactor Institute, Kyoto University

INTRODUCTION: In recent years various types of coherent radiation emitted from a short bunch of relativistic electrons have attracted a considerable attention as a bright light source in the THz-wave and millimeter wave regions for the spectroscopic purpose. Coherent transition radiation (CTR), which is emitted from a boundary between two media, is one of such a coherent light source. CTR is usually utilized as a non-polarized light source, because the electric vector of transition radiation (TR) emitted from a metallic screen is axially symmetric with respect to the trajectory of an electron beam. In my previous reports [1] the circularly polarized CTR using a pair of wire-grid radiators with the different polarization has been developed with a new idea. The significant point of my new technique is the use of linearly polarized CTR with the wire-grid radiator. With this technique the polarization degree is able to be controlled precisely. Circularly polarized light has been useful in the circular dichroism spectroscopy. In this report spectra of some kinds of amino acid have been measured using linearly polarized CTR.

EXPERIMENTAL PROCEDURES: The experiment was performed at the coherent radiation beamline [2] at the L-band linac of the Research Reactor Institute, Kyoto University. The energy, the width of the macro pulse, and the repetition rate of the electron beam were 42 MeV, 47 ns, and 60 Hz, respectively. The average current of the electron beam was 2.3 μA. The spectrum of CTR was measured by a Martin-Puplett type interferometer and a liquid-helium-cooled Si bolometer. The schematic diagram of the experiment was shown in Fig.1.

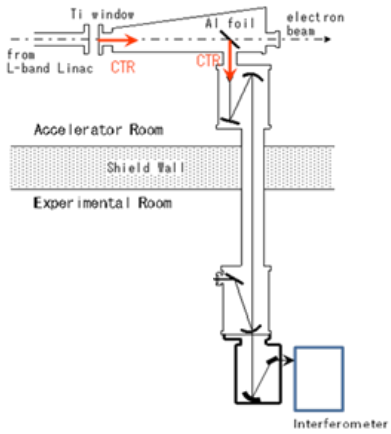

Fig. 1 The schematic diagram of the experiment.

RESULTS: Measured spectra of some kinds of amino acid, e.g., Phenylalanine, α-Alanine, and Tryptophan, are shown in Figs. 2. Difference between L and D forms has been observed. The identification of observed absorption is now in progress.

REFERENCES:

[1] T. Takahashi, *et al.*, KURRI-PR 2015 CO4-7.

[2] T. Takahashi *et al.*, Rev. Sci. Instrum. **69** (1998) 3770.

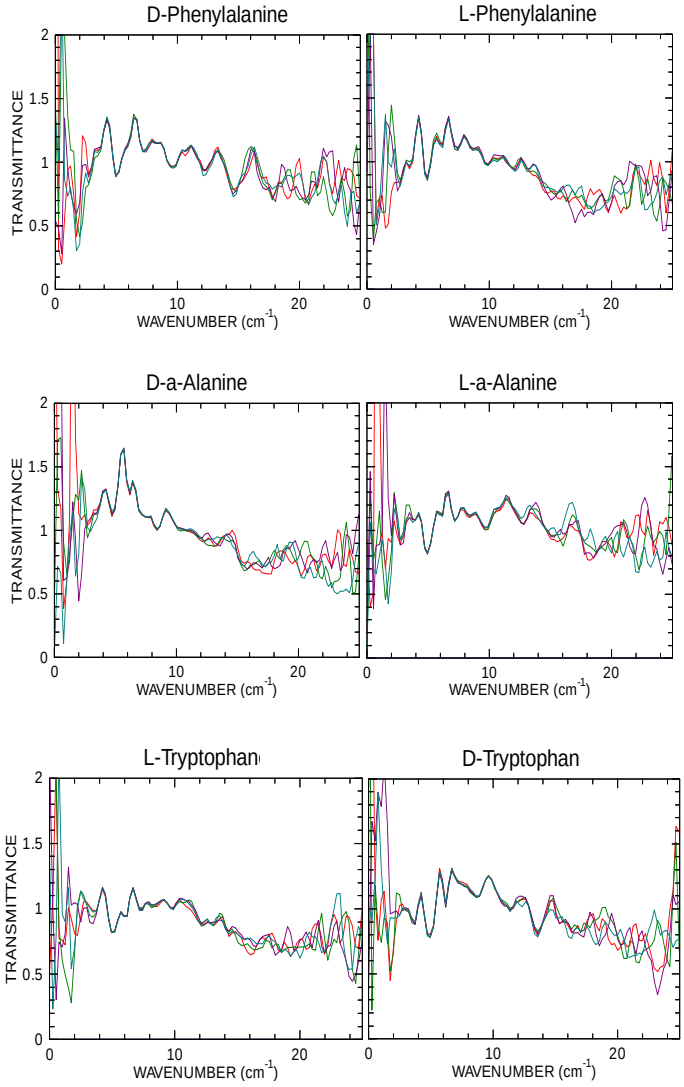

Fig. 2 Spectra of some kinds of amino acid.

CO4-9 Complex Structure of Ions Coordinated with Hydrophilic Polymer. 17. Inner Precipitation of Inorganic Salt as Fillers and Their Dissolution.

A. Kawaguchi and Y. Morimoto

Research Reactor Institute, Kyoto University

INTRODUCTION: We have reported interacted structures between iodine (polyiodide ions, I_n^{m-}, *m*, *n*: integer, $n \neq 1$) and polymers.[1] Even if polyiodide ions are prepared as solutes in aqueous solution, they can be diffused into various polymeric matrix, both to hydrophilic polymers and to hydrophobic ones through easy operation at room temperature. Such preparation is expected to introduce novel functionality and wide applications to polymeric materials with easy operation.[2]
On the other hand, results applied with "inner precipitation" can not be easily controlled in some cases. As one reason, it is due to spontaneous ionic diffusion from outer solution of free transfer of ions into polymeric environment with restriction on ionic diffusion and due to inner ionic diffusion under hierarchic structure of polymers and uncertainty of polyiodide ions. Under such complication and diversity, posterior ionic diffusion represented as "secondary doping" of Ag^+ ion or other metallic ions is expected to indicate different scheme of ionic diffusion or their reaction different from ones in solution.
And, for precipitation or production of AgI, which is hardly soluble inorganic salt in water, it also shows unusual behavior against independent ordinary powder of the salt.

EXPERIMENTS: Sample preparation for hydrophilic polymer (PA6, polyamide-6, Nylon™-6, TORAY) and hydrophobic matrix (“SEBS”- elastomer, ARON-KASEI Co.Ltd.) was mentioned before.[3,4]
"Rayfan #1401" in thickness of 0.1mm was used as non-doped PA6. A strip cut from a PA6 sheet were stretched (x3-4) and was annealed at 210˚C in vacuum. This strip was doped with I_2-KI(aq) (0.2N) at 5˚C for more than 5days and this process (iodine-doping) was terminated by rinsing with water. After drying in vacuum at R.T.(25˚C) for 3 weeks, the sample was immersed in $AgNO_3$(aq) (2M) at R.T. for more than 24hrs.
As hydrophobic materials as matrix, commercial "SEBS"-elastomer, AR-770C and AR-830C were used as hydrophobic matrixes, which are composed of both polystyrene (hard segment) and polyethylene-polybutylene co-polymer (soft segment). Iodine doping for these hydrophobic matrixes was achieved with I_2-KI(aq)/3.0N (for 22 hrs., at R.T.) and secondary doping of Ag^+ ion was done with $AgNO_3$(aq)/0.25M (for 30min., at R.T.).

RESULTS: Iodine (I_2) is insoluble to water. Therefore, for preparation of aqueous solution of I_3^-, which is the smallest polyiodide ion, mono-iodide ion (I^-) is required for polyiodide ions tosolve in aqueous solution. On the other hand, prior existence of I^- ion produces precipitation of silver iodide (AgI) salt on posterior addition of Ag^+ ion. ($Ag^+ + I^- \rightarrow AgI\downarrow$) In the case of aqueous solution of polyiodide ion or "(1st) iodine-doped" hydrophilic polymers (for example, I_2-KI(aq) or "iodine-doped" PA6 or "iodine-doped" PVA, etc.), posterior addition of Ag^+ ion forms precipitation of AgI nano-grains; inner diffusion of Ag^+ ion ("secondary doping") into "iodine doped" hydrophilic polymers can realize "as-shaped" hybrid composite where fillers of inorganic salt grains are dispersed in hydrophilic matrixes.[5]
However, while independent AgI grains are stable at room temperature and show very low solubility in water, AgI precipitates dispersed in polymeric matrixes which are prepared as "as-shaped" composite are not always stable nor unchanged. Inner precipitation of AgI grains in PA6 matrix also shows activity to swelling; dissolution of the *"hardly soluble" salt* by water swelling is observed in SANS profiles.[6] And even for as hydrophobic matrix, such as "SEBS"-elastomer, inner dispersion of Ag^+ ion and dissolution of AgI or polyiodide ions are also observed.[7] Generally, there is tendency that excessive "secondary doping" induces dissolution of AgI precipitates.
It is one evidence to indicate that Ag^+ ion can be posteriorly diffused into hydrophobic matrixes from aqueous solution, and that inner precipitation of AgI which temporally formed in the matrixes can be easily dissolved or released with advance of "secondary doping". On considering application or functionality on surface of polymeric materials applied with "iodine-doping", suggested as metallic plating for example, such antinomic process should be also considered.

REFERENCES:

[1] A. Kawaguchi, Polymer, **35**, 3797-3798. (1994)
[2] patent. JPN-5444559 (2014).
[3] A. Kawaguchi, *et.al.,* KURRI Prog. Rep. 2010, 218-218. (2011)
[4] A. Kawaguchi, *et.al.*, KURRI Prog. Rep. 2014, 114-114. (2015)
[5] A. Kawaguchi, *et.al.*, Polym. Prep. Jpn., **56**, 769-769. (2007)
[6] A. Kawaguchi, *et.al.*, KURRI Prog. Rep. 2002, 20-20. (2003)
[7] A. Kawaguchi, Polym. Prep. Jpn., **60**, 630-630. (2011)

CO4-10 Hydrogen Retention on plasma Facing Material Irradiated by High Energy Particle Beam

K. Tokunaga, M. Matsuyama[1], K. Araki, M. Hasegawa, K. Nakamura and Q. Xu[2]

Research Institute for Applied Mechanics, Kyushu University
[1]Hydrogen Isotope Research Center, University of Toyama
[2]Research Reactor Institute, Kyoto University

INTRODUCTION: It is of importance to clarify phenomena of implantation, retention, diffusion and permeation of tritium on surface of the armor materials of the first wall/blanket and the divertor on fusion device from a viewpoint of precise control of fuel particles, reduction of tritium inventory and safe waste management of materials contaminated with tritium (T). Refractory metals such as tungsten (W) is potential candidate for an armor of the first wall and the divertor plate of the fusion reactor because of its low erosion yield and good thermal properties. The armor material will be subjected to heavy thermal loads in the steady state or transient mode combined with high energy neutron irradiation that will cause serious material degradation. In addition, high energy runaway electrons would bombard the armor materials along the equatorial plane in fusion device. It is considered that these cause radiation damage and enhance tritium retention. In the present works, T exposure experiments have been carried out on W samples which were irradiated by high energy electrons using LINAC in KURRI of Research Reactor Institute, Kyoto University to investigate effects of high energy electrons irradiation and microstructure on tritium retention of W. In this fiscal year, pure W and recrystallized W were irradiated by high energy electron beam. After that, positron annihilation experiment was carried out to identify the radiation defect. In addition, tritium exposure experiments have been carried out using a tritium (T) exposure device.

EXPERIMENTS: W samples used were ITER grade W (IG-W) and recrystallized W. In the case of IG-W, one was W sample (ITER grade W(1)) which the surface were manufactured to be oriented parallel to the rolling surface and rolling direction. The other W sample (ITER grade W(3)) which the surface were manufactured to be oriented perpendicular to the rolling surface and rolling direction. On the other hand, heat treatment was performed at 1800 ºC for 1h at high vacuum to recrystallize IG-W. The sizes of W samples were 10mm x 10mm x 1mm. The surface of the both samples were polished to be mirrored. High energy electrons irradiation has been carried out using LINAC in KURRI of Research Reactor Institute, Kyoto University. An energy of electron irradiated was 10 MeV and DPA was 2.8 x 10^{-3}. Temperature during the irradiation was measured by thermocouples which was contacted with a backside of the W samples. After the electron beam irradiation, positron annihilation experiment was carried out. In addition, T exposure experiments have been carried out using a T exposure device in University of Toyama. Pressure of the T gas was 1.3 kPa and T exposure was kept for 4 h. T concentration in the gas was about 5 %. Temperatures of pre-heating and T exposures were 100 ºC. After the exposure to T gas, T amount retained in surface layers of the sample was evaluated by β-ray-induced X-ray spectrometry (BIXS) and imaging plate (IP) measurements.

RESULTS: As shown in Fig. 1, there is little difference between results from W(1) and W(3). On the other hand, after the recrystallization, lifetime from defect (τ_2) increased and intensity of I_2 decreased. This result indicates that defects of the small number with large clusters were formed by the recrystallization. The electron irradiation made life time of τ_2 small. In addition, intensity of I_2 increased. These indicate that small defects were induced and concentration of the defects increased both of pure W and recrystallized W by the electron irradiation. T exposure experiments have been carried out and impact on the electron beam irradiation of T retention is under investigation.

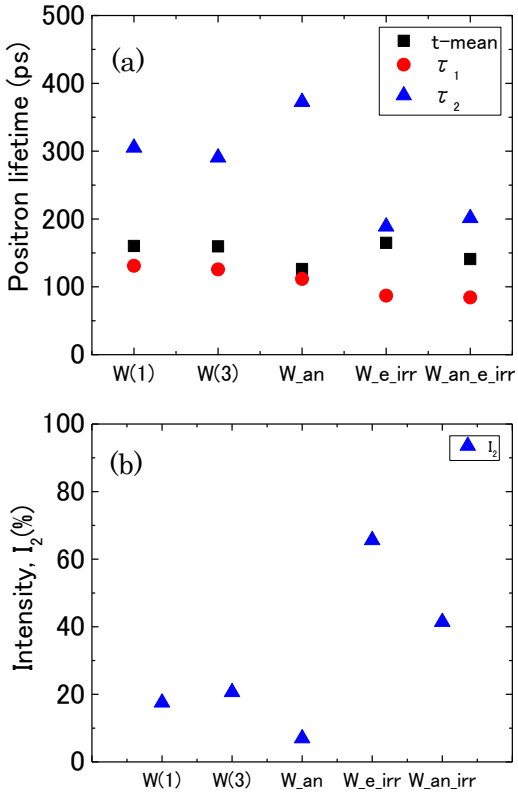

Fig. 1. Positron life time(a) and intensity of I_2 (b). W_an is the sample which was recrystallized. W_e_irr and W_an_ii are electron irradiated samples of pure W and recrystallized W, respectively.

CO4-11 Presence of Diluted High-valence Fe and Sn Ions in Layered Rock-salt Structure

M. Tabuchi and Y. Kobayashi[1]

National Institute of Advanced Industrial Science and Technology (AIST)
[1]Research Reactor Institute, Kyoto University

INTRODUCTION: Although the Fe ion in iron oxides has 2+ and/or 3+ states, tetravalent and pentavalent Fe ion can be stabilized in Perovskite structure. Tabuchi et al. found tetravalent Fe ion in $LiFeO_2$-Li_2MnO_3 solid solution with layered rock-salt structure (*R*-3*m*) at 15 years ago [1] using ^{57}Fe Mössbauer spectroscopy. He detect also pentavalent Fe ion in the solid solution below 10K [2]. Through long-term efforts to brush-up synthetic method, this material is now attractive one as high-capacity positive electrode material [3, 4].

In this work, $0.2LiFeO_2$-$0.8Li_2MnO_3$ solid solution was selected using different synthetic procedure. We succeeded to find hexavalent iron by low-temperature ^{57}Fe Mössbauer measurements. Although the hexavalent iron can be stabilized at only tetrahedral site, X-ray Rietveld analysis was done.

EXPERIMENTS: The $0.2LiFeO_2$-$0.8Li_2MnO_3$ sample was prepared by coprecipitation-calcination method. $Fe(NO_3)_3 \cdot 9H_2O$ and $MnCl_2 \cdot 4H_2O$ reagents dissolved with distilled water. The Fe-Mn aq. soln. (Fe:Mn molar ratio=2:8) was dripped into NaOH solution at 20 °C for 2-3 h. The Fe-Mn coprecipitate was oxidized by bubbling with oxygen for 2 days. After washing and filtration, aged Fe-Mn coprecipitate was dispersed into LiOH soln. (Li/(Fe+Mn)=2.00). The slurry was dried at 50 °C for 2 days and then the dried mixture was pulverized for calcination. The mixture was firstly calcined at 500°C for 20h under O_2 flow and then fired at 700 or 750 °C for 20h in O_2 or N_2 flow. All products were washed with distilled water, filtered and dried at 100 °C for above characterization.

RESULTS: Fig. 1 shows ^{57}Fe Mössbauer spectra at 3 K for two samples calcined at different temperature in O_2 flow. The spectra were analyzed by same fitting model: three sextets and one symmetric doublet with different isomer shifts (IS). A sextet with the largest internal field (H_i=45-46 T) is assigned as high-spin trivalent iron because of its IS value (+0.42-+0.43 mm/s). Other two sextets have almost the same IS value (+0.20-+0.21 mm/s) and different H_i values (12 and 22T). These parameters indicated that tetravalent irons with two kinds of local structure existed. The origin is still unknown. Surprisingly, the IS value for the doublet (IS=-0.73 mm/s) was quite small, which can be assigned as hexavalent iron like $BaFeO_4$. To the best of our knowledge, this is the first time to detect hexavalent Fe in complex oxides. Since the hexavalent iron can be stabilized at tetrahedral site, careful X-ray Rietveld analysis was performed.

The analysis showed that transition metals existed not only typical four octahedral 4*g*, 2*b*, 2*c* and 4*h* sites but also tetrahedral 8*j* one (5-7 % in occupancy) in monoclinic layered rock-salt structure (*C*2/*m*). As shown in Fig. 2, the $M_{8j}O_4$ tetrahedron adjacent to $M_{4g}O_6$ octahedron was highly distorted; they consisted of three short M_{8j}-O distances and one long M_{8j}-O one. In addition to the above analysis, low-temperature XRD data have to be taken, because the hexavalent iron cannot be detected at 300 K.

After finishing the above analysis, Sn doped samples will be prepared, because tin doped sample is attractive to improve the electrochemical cycle performance.

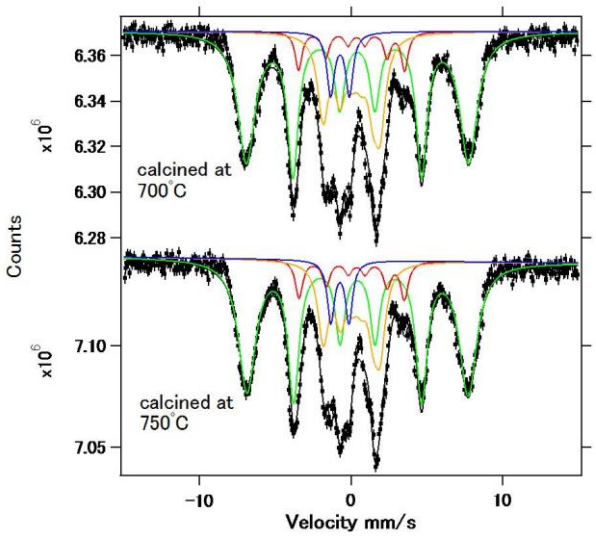

Fig. 1 ^{57}Fe Mössbauer spectra at 3 K for two samples calcined at 700 (upper) or 750 °C (lower part) in O_2 flow.

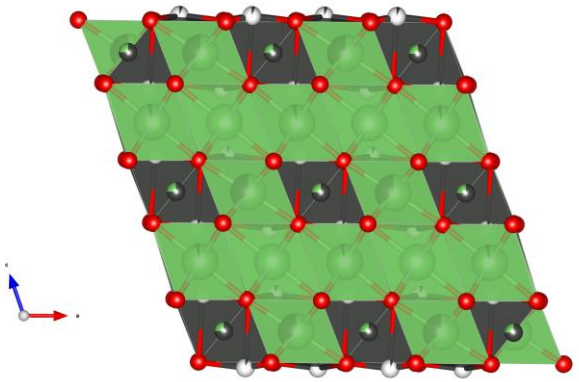

Fig. 2 Applied cation distribution model for X-ray Rietveld analysis. Gray circles correspond to cation on tetrahedral 8*j* site.

REFERENCES:

[1] M. Tabuchi *et al.*, J. Electrochem. Soc., **149** (2002) A509-A524.
[2] M. Tabuchi *et al.*, J. Appl. Phys., **104** (2008) 043909-1-10.
[3] M. Tabuchi *et al.*, J. Power Sources, **318** (2016) 18-25.
[4] M. Tabuchi *et al.*, J. Power Sources, **195** (2010) 834-844.